Citation: Molecular Therapy—Nucleic Acids (2016) 5, e288; doi:10.1038/mtna.2016.6
Official journal of the American Society of Gene & Cell Therapy
www.nature.com/mtna

DNA as Tunable Adaptor for siRNA Polyplex Stabilization and Functionalization

Philipp Heissig[1], Philipp M. Klein[1], Philipp Hadwiger[2] and Ernst Wagner[1]

siRNA and microRNA are promising therapeutic agents, which are engaged in a natural mechanism called RNA interference that modulates gene expression posttranscriptionally. For intracellular delivery of such nucleic acid triggers, we use sequence-defined cationic polymers manufactured through solid phase chemistry. They consist of an oligoethanamino amide core for siRNA complexation and optional domains for nanoparticle shielding and cell targeting. Due to the small size of siRNA, electrostatic complexes with polycations are less stable, and consequently intracellular delivery is less efficient. Here we use DNA oligomers as adaptors to increase size and charge of cargo siRNA, resulting in increased polyplex stability, which in turn boosts transfection efficiency. Extending a single siRNA with a 181-nucleotide DNA adaptor is sufficient to provide maximum gene silencing aided by cationic polymers. Interestingly, this simple strategy was far more effective than merging defined numbers (4–10) of siRNA units into one DNA scaffolded construct. For DNA attachment, the 3′ end of the siRNA passenger strand was beneficial over the 5′ end. The impact of the attachment site however was resolved by introducing bioreducible disulfides at the connection point. We also show that DNA adaptors provide the opportunity to readily link additional functional domains to siRNA. Exemplified by the covalent conjugation of the endosomolytic influenza peptide INF-7 to siRNA via a DNA backbone strand and complexing this construct with a targeting polymer, we could form a highly functional polyethylene glycol–shielded polyplex to downregulate a luciferase gene in folate receptor–positive cells.

Molecular Therapy—Nucleic Acids (2016) **5**, e288; doi:10.1038/mtna.2016.6; published publication 1 March 2016
Subject Category: nucleic acids chemistries

Introduction

RNA interference (RNAi) was discovered in 1998 as a mechanism for gene regulation on the mRNA level by small RNA.[1] The most popular exponents are siRNA and microRNA. In their active form, both are short double-stranded RNAs (21 base pairs (bp)), which guide gene silencing through complementarity to their target mRNA.[2–5] The capability of siRNA to specifically knockdown a gene of interest holds a huge therapeutic potential, and plenty of research is focused on its efficient delivery to its target site.[5–9] A well-studied approach in nonviral gene therapy is the complexation of nucleic acids with cationic polymers.[10–12] Due to its small size, siRNA generally forms less stable inter-electrolyte complexes than plasmid DNA.[13] Increasing the size and charge density of siRNA is therefore an option to tackle this problem and hence to increase its transfection efficiency. Short DNA overhangs are known to have a positive effect on cellular uptake.[14] Larger assemblies can be achieved by other approaches such as noncovalent polymerization of siRNA via sticky ends[15] or employing disulfide chemistry.[16,17] The number of siRNA units in such multimeric assemblies is largely not well defined. A strategy commonly pursued is the formation of larger defined structures containing multiple siRNA units.[18–20] DNA oligomers can be used as a framework to merge several siRNA units into one construct.[21,22] DNA is especially suitable for this purpose as it is simply accessible and a huge variety of structures can be assembled by Watson Crick base pairing. As DNA is a natural molecule, it can be degraded by endogenous pathways and consequently toxicity is deemed unlikely.[23,24] From simple structures such as polyhedrons[25–27] up to very complex designs using the DNA origami approach,[28–30] various different shapes have been established from which only a few have been tested for siRNA delivery. Examples include a DNA tetrahedron or a DNA nanotube conjugated to siRNA and folate, which could be delivered to folate receptor–bearing cells.[31,32]

The current work provides an overview of how DNA adaptor molecules can be used to improve cellular delivery of siRNA in polyplexes employing sequence-defined cationic polymers. These polymers[33] possess protonable amines and optionally additional functional units like targeting ligands,[34] shielding,[35] and endosomolytic domains[36] to overcome the barriers for efficient DNA/RNA transfer to the target cell. DNA oligonucleotides provide versatile opportunities for extension, multimerization, and functionalization of siRNA, which we studied in a comparative way. The idea was to figure out which parameters are of importance with respect to polyplex formation and transfection efficiency.

A siRNA connected via the 3′ end of the passenger strand to a 181-nucleotide adaptor DNA extension turned out to be the best transfecting construct, whereas merging multiple siRNA units into one construct was less effective. Additionally, the endosomolytic influenza peptide INF-7[37] could be

[1]Pharmaceutical Biotechnology, Department of Pharmacy, Center for Nanoscience, Ludwig-Maximilians-Universität, Munich, Germany; [2]Axolabs GmbH, Kulmbach, Germany. Correspondence: Ernst Wagner, Pharmaceutical Biotechnology, Department of Pharmacy, Center for Nanoscience, Ludwig-Maximilians-Universität, Butenandtstr. 5-13, Haus D, 81377 München, Germany. E-mail: ernst.wagner@cup.uni-muenchen.de
Keywords: DNA nanostructures; nucleic acid delivery; polyplex; RNA interference; siRNA
Received 8 October 2015; accepted 13 January 2016; published publication 1 March 2016. doi:10.1038/mtna.2016.6

successfully connected to siRNA via a DNA adaptor resulting in a folate-targeted, polyethylene glycol (PEG)–shielded polyplex with high gene silencing efficiency.

Results

DNA backbone for siRNA extension

The basic structure used for this approach is composed of two siRNAs directed against eGFP linked by a 79-nucleotide DNA backbone strand. In detail, the siRNA consists of a chemically modified guide strand and a chemically modified complementary passenger strand with either a 5′ or a 3′ 18-nucleotide DNA extension. Via the extensions, the siRNAs are hybridized to both ends of the DNA backbone strand resulting in structure 1bb2si (= 1 backbone strand + 2 siRNAs) (**Figure 1a**). The sequences for all oligonucleotides used in this work can be found in **Supplementary Table S1**. The construct is formed by mixing the components in their respective molar amounts, heating to 95 °C, and slow cooling to room temperature (RT). The assembly of the construct is accomplished by building the structure from its subunits and monitoring the retention of each by native polyacrylamide gel electrophoresis (PAGE). All assemblies were clean and showed the expected difference in migration (**Figure 1b**). For transfection, the nanostructure was complexed with the three-armed cationic polymer 689.[36] Each arm contains three protonable succinoyl tetraethylene pentamine (Stp) units for complexation of the negatively charged nucleic acids, four histidines that promote endosomal escape through the proton-sponge effect,[38] and terminal cysteines for polyplex stabilization through disulfide bond formation (**Figure 1c**). To test whether 1bb2si has already advantages over a canonical siRNA format in transfection-mediated gene silencing experiments, it was mixed with polymer 689 at an amine to phosphate ratio of 6 (N/P ratio of 6, including all phosphates from siRNA and DNA) and transfected into murine neuroblastoma N2A/eGFPLuc cells that stably express an eGFP–luciferase fusion protein in medium supplemented with 10% fetal bovine serum (FBS).

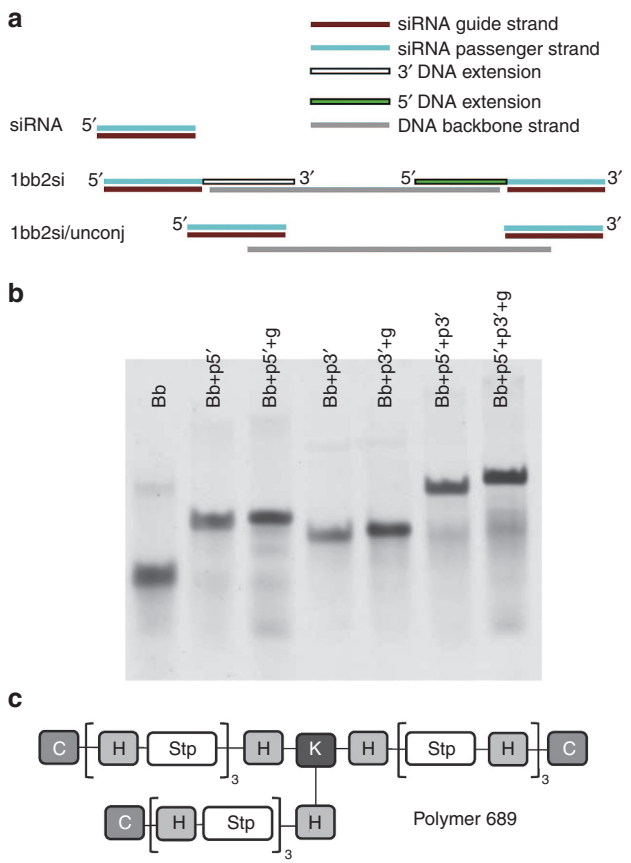

Figure 1. Assembly of DNA nanostructures for polyplex formation. (**a**) Basic building block consisting of two siRNAs with a DNA extension at the 3′ or 5′ terminus of the passenger strand used for hybridization to both ends of a DNA backbone strand (1bb2si). Unconjugated control consisting of two equivalents siRNA mixed with one equivalent backbone strand (1bb2si-unconj). (**b**) Assembly of 1bb2si from its subunits verified on a native polyacrylamide gel (Bb: DNA backbone strand; p5′: passenger strand with 5′ DNA extension; p3′: passenger strand with 3′ DNA extension; g: guide strand, gel cropped). (**c**) Polymer 689 for complexation of the DNA nanostructures (C: cysteine; H: histidine; Stp: succinoyl tetraethylene pentamine; K: lysine, structure from N to C).

Luciferase is downregulated upon gene silencing of the eGFPLuc fusion mRNA and represents a convenient quantitative readout for subsequent transfections. The siRNA was used at a concentration of 0.36 µM, and the polyplexes were incubated on the cells for 48 hours. Luciferase knockdown is specified as relative to a buffer-treated cell control. As expected, the canonical siRNA already exhibited a high gene silencing efficiency, but it was outperformed by 1bb2si. A control was included to verify that the hybridization of the siRNA to the DNA backbone strand is necessary. siRNA without DNA extensions was mixed with the respective amount of the DNA backbone strand (1bb2si-unconj). Silencing by 1bb2si-unconj was comparable with that of the canonical siRNA. Thus the beneficial effect of the nanostructure cannot be achieved by mixing siRNA with DNA without prior conjugation of complementary DNA extensions (**Figure 2a**). To challenge the effectiveness of 1bb2si, the incubation time was decreased to 1.5 hours and the siRNA concentration was reduced to 0.2 µM. While gene silencing of 1bb2si remained as good as in the previous experiment, the efficiency of the canonical siRNA as well as of 1bb2si-unconj was significantly reduced (**Figure 2b**).

To examine whether the enhanced transfection efficiency is due to the formation of more stable polyplexes, a comparative binding assay of canonical siRNA and 1bb2si at different N/P ratios was performed on an agarose gel. After complexation, charge neutralized particles remain in the pocket while free nucleic acids migrate into the gel. For 1bb2si, the retention was nearly complete already at N/P ratio of 3, indicating that only a low polymer excess is necessary to form stable polyplexes proofing complete binding of the construct. In contrast, with canonical siRNA even at a N/P ratio of 24 still free siRNA could be detected (**Figure 2c**).

Influence of polymer and siRNA concentration

The previous transfections were conducted at a constant N/P ratio of 6. As extension of siRNA with DNA comes along with an increase in phosphates per unit, the amount of polymer used for complexation of 1bb2si was higher than for siRNA. To exclude that the positive effect is due to the increase in polymer amount, the transfections were repeated at constant

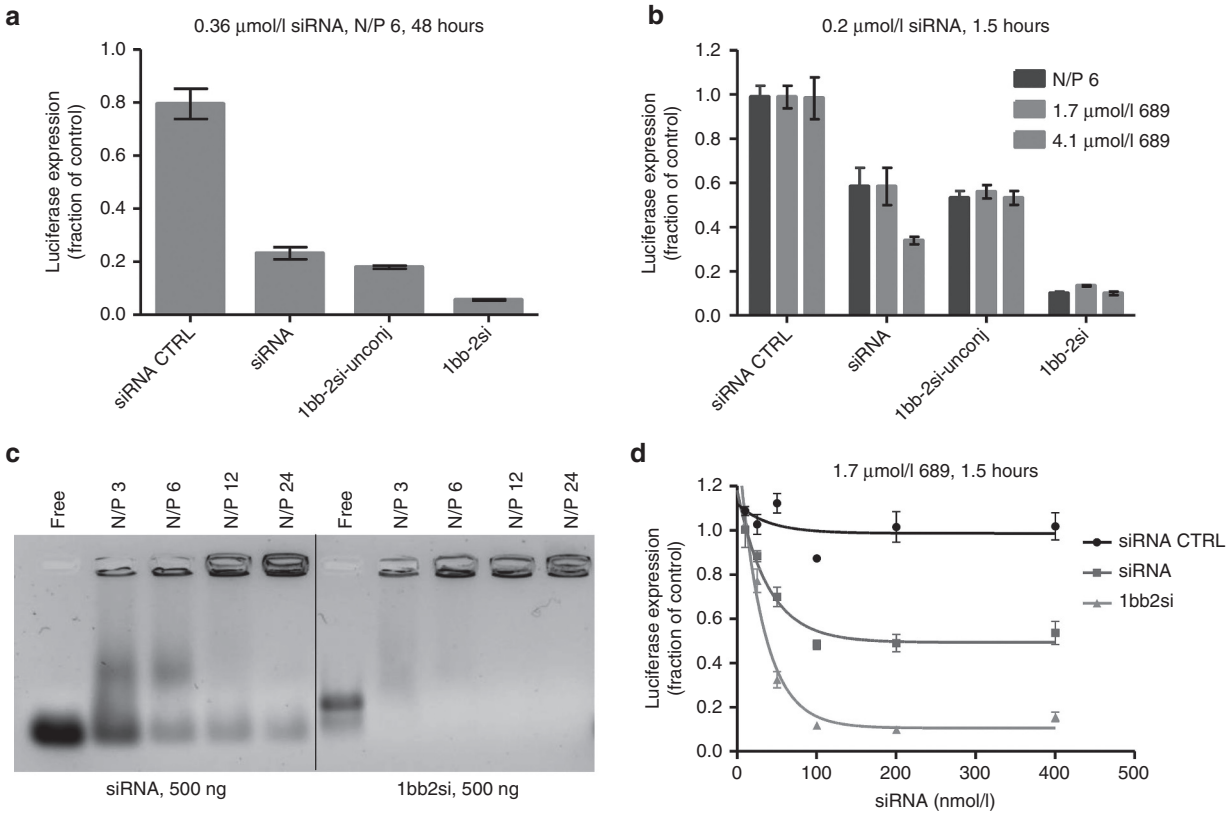

Figure 2. Transfection efficiency and stability of polyplexes formed with polymer 689 and siRNA, 1bb2si or 1bb2si-unconj. (**a**) eGFP–luciferase knockdown in N2A/eGFPLuc cells with 0.36 µM anti-eGFP siRNA at N/P ratio of 6 and 48 hours of incubation time. (**b**) Comparison of eGFP–luciferase knockdown at constant N/P ratio and constant polymer concentration with 0.2 µM siRNA and 1.5 hours of incubation time. (**c**) Binding assay for canonical siRNA and 1bb2si at different N/P ratios. Complexed nucleic acids remain in the loading pocket while free nucleic acids migrate into the gel (gel cropped). (**d**) Correlation of gene silencing with siRNA concentration. Data are presented as mean ± SD.

polymer concentrations of 1.7 and 4.1 µM (corresponding to a N/P ratio of 6 for both, the canonical siRNA and 1bb2si). In both cases, the prior results could be reproduced (**Figure 2b**). Considering this fact, subsequent transfections were conducted at a constant polymer concentration of 1.7 µM.

To examine the influence of the siRNA concentration, the amount of 1bb2si and canonical siRNA was varied and transfection efficiency was compared. The maximal reduction of luciferase expression was achieved for both samples at 0.1 µM (siRNA 50%, 1bb2si: 10%). A further increase in concentration had no effect (**Figure 2d**). This proves that the gene silencing efficiency of 1bb2si cannot be achieved by raising the siRNA concentration. Within the examined range, the advantage of 1bb2si over canonical siRNA is independent of N/P ratio, polymer, and siRNA concentration.

Complex or simple structures?

More sophisticated multimeric siRNA structures can easily be formed with the building block 1bb2si (**Figure 3**). By annealing three of these constructs through their DNA backbone, a three-armed structure containing six siRNA units was assembled (3bb6si). A five-armed structure containing 10 siRNA units was constructed by the same strategy (5bb10si) and a four-armed structure with only one siRNA per arm was assembled by linking two 1bb2si building blocks by two DNA backbone strands (4bb4si).

The larger constructs were less defined on a native PAGE gel (**Supplementary Figure S1**) and also transfection efficiency decreased with increased number of siRNA units per structure (**Supplementary Figure S2**).

Hence, the next step was to consider more simple structures than 1bb2si, which can be achieved by testing the subunits of 1bb2si for gene silencing (**Figure 4a**). This provides also an insight into the possible cause of the enhanced transfection efficiency of 1bb2si. Constructs extended by 18 DNA nucleotides either at the 3′- or 5′-end of the passenger strand (siRNA/3′ov, siRNA/5′ov) are already slightly more efficacious compared with canonical siRNA. However, hybridizing either of the two constructs separately to the DNA backbone strand (1bb1si/3′ov and 1bb1si/5′ov, respectively) boosts transfection efficiency even more. Single siRNA construct 1bb1si/3′ov performs equally well as dimer siRNA construct 1bb2si (**Figure 4b**). This indicates that attaching more siRNAs to one structure is not necessarily beneficial. It can even be detrimental as shown in the previous experiment (**Supplementary Figure S2**). What seems to matter is an extension of a single siRNA by adaptor DNA. Regarding the attachment site of the DNA extension, the 3′ extended structures exhibited an increased gene silencing efficiency

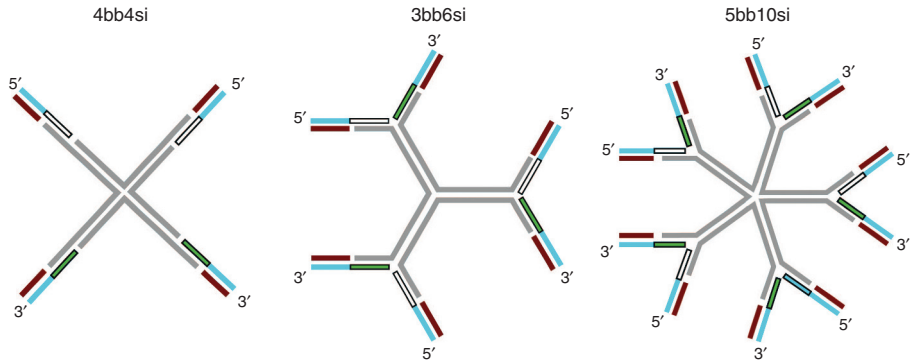

Figure 3. Design of star-shaped multi-siRNAs. Nanostructures containing 4, 6, or 10 siRNA units were assembled from 1bb2si building blocks.

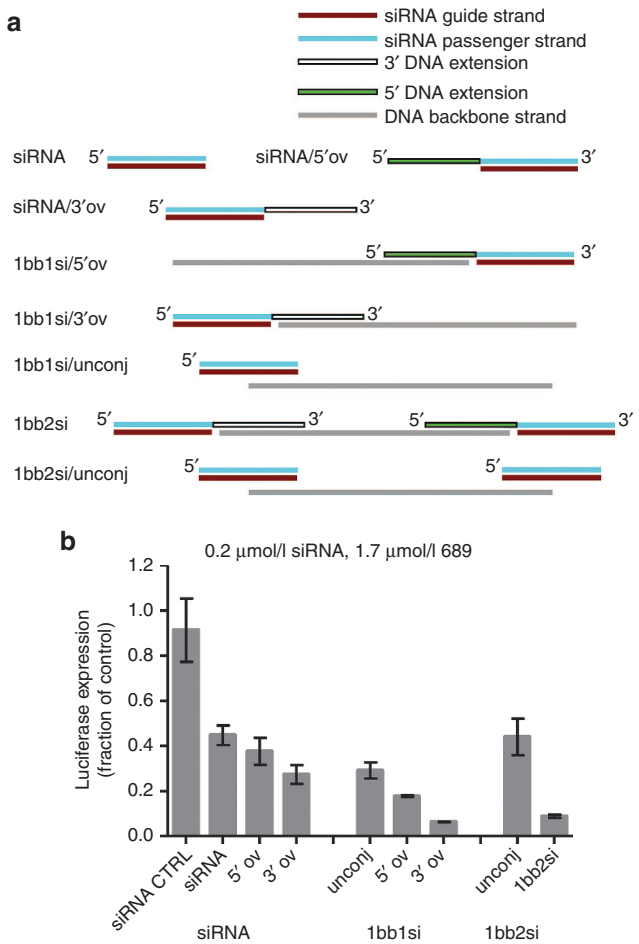

Figure 4. Transfection efficiency of the subunits of 1bb2si. (**a**) Schematic representation of the subunits of 1bb2si and (**b**) luciferase knockdown after complexation with polymer 689. Canonical siRNA and 1bb2si were compared with the 5′ or 3′ passenger strand extended constructs with and without hybridization to the DNA backbone strand. The unconjugated controls consist of siRNA lacking the DNA extensions and DNA backbone strand mixed in equimolar amounts.

compared with their 5′ counterparts. All substructures of 1bb2si possess single-stranded DNA regions of different length (siRNA/3′ov: 18 bases, 1bb2si: 43 bases, 1bb1si/3′ov: 61 bases). As single strands are more flexible than double strands, this might be a requirement for stable particle formation and hence increased transfection efficiency. To test this hypothesis, the respective double-stranded equivalents were assembled and examined for luciferase knockdown with polymer 689 (siRNA/3′ov-ds, 1bb1si/3′ov-ds, 1bb2si-ds, **Supplementary Figure S3**). siRNA/3′ov-ds and 1bb2si-ds and their single-stranded counterparts resulted in a similar silencing efficiency, indicating that a single-stranded domain is not a requirement. In contrast, 1bb1si/3′ov-ds showed a reduced knockdown. The stiffness of its long unnicked double strand might destabilize polyplexes.

Optimal length of DNA sequence per siRNA

Given the results above, we asked the question whether there is an optimum DNA sequence length connected to a single siRNA. Due to a better transfection efficacy of DNA extension at the passenger strand's 3′-terminus compared with the 5′-counterparts, we decided to probe a potential DNA sequence length bias with a sequential DNA extension approach. DNA strands with a complementary part to the previous extension and a 20-nucleotide part for further extension were used to assemble the different sized defined structures (Ext I, Ext II, Ext III, Ext IV, Ext V; **Figure 5a**). The assembly of the constructs was verified by native PAGE (**Figure 5b**). We observed a positive correlation of gene silencing efficiency and construct size. siRNA/3′ov with a single-stranded DNA overhang displays improved silencing activity as compared with canonical siRNA without overhang. Double-stranded DNA extensions up to Ext II resulted in strong increase in potency. Larger constructs (Ext III to V) did not increase transfection efficiency further (**Figure 5c**). This indicates that in this setup, conjugation of a single siRNA to an at least 99-nucleotide DNA extension provides the maximum silencing effect. As all constructs contain a similarly long stretch of 20-nucleotide single-stranded DNA, the positive effect of flexible single-strandedness on polycation complexation can be ruled out as major cause for the enhancement.

Reducible versus nonreducible siRNA attachment

In all previous experiments, irrespective of the siRNA's terminus, the DNA extension is covalently connected to the passenger strand via a phosphodiester linkage. It is possible that this chemistry prevents the siRNA from gaining full activity. This

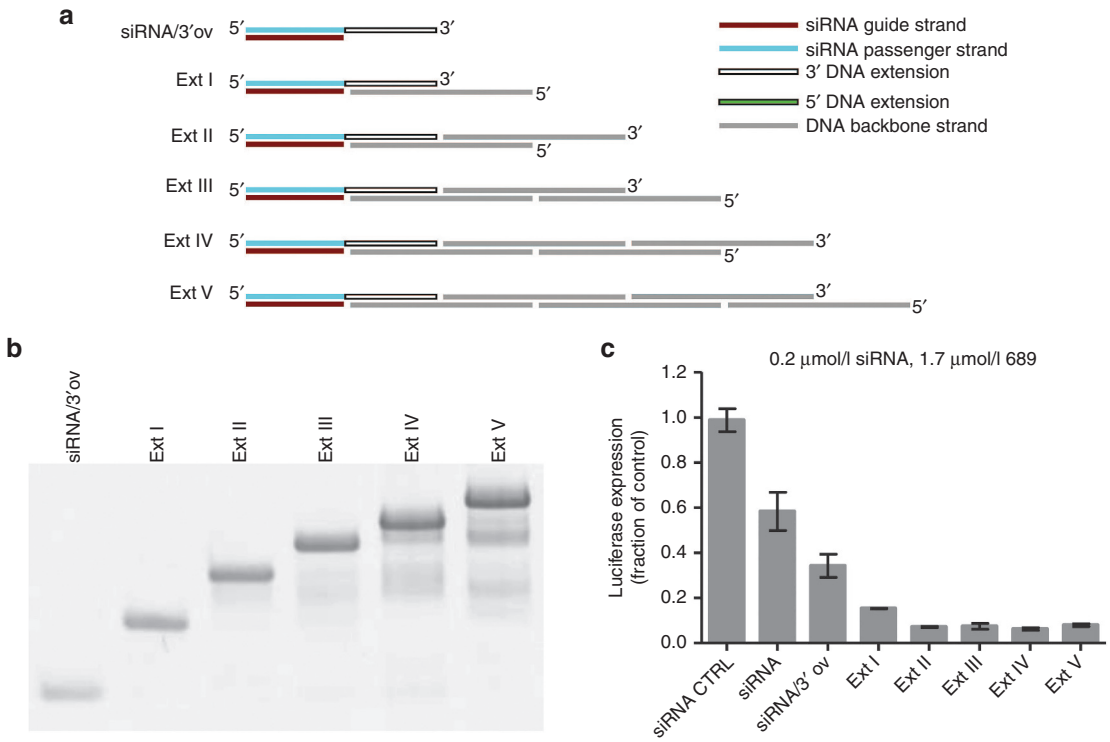

Figure 5. Optimal sequence length of DNA backbone. (**a**) Schematic representation of the stepwise DNA extended siRNA. Each extension step is accomplished by a DNA strand with one segment complementary to the previous extension and a 20-nucleotide segment for further extension. (**b**) Assembly (verified by native polyacrylamide gel electrophoresis, gel cropped) and (**c**) transfection efficiency of the nanostructures.

assumption is supported by the difference in efficiency of the 5′ and 3′ extended passenger strand. To test this hypothesis, we engineered a biocleavable disulfide linker between the RNA and the DNA extension sequence. We wanted to utilize the cytosol's reducing environment to cleave the disulfide bond, which should leave the siRNA in a more accessible form for the RNA-induced silencing complex (RISC).

In order to implement this strategy, we used two thiol modified 18-nucleotide DNA strands, each complementary to one end of the 79-nucleotide backbone strand that was used for the assembly of 1bb2si. An eGFP-siRNA with a 5′ thiolated passenger strand was activated with 5,5′-dithiobis-(2-nitrobenzoic acid) and coupled to the thiolated DNA strand. The respective constructs from the previous experiments were assembled using the disulfide-extended siRNA (SS-1bb1si/5′ov, SS-1bb1si/3′ov, SS-1bb2si) (**Figure 6a**). Verification of the structures was again performed with native PAGE (**Figure 6b**). All three structures showed a very efficient gene silencing activity similar to the one of 1bb2si (**Figure 6c**). In contrast to the previous experiments, the DNA extensions are attached to the 5′ end of the siRNA passenger strand. The decreased silencing potential observed for the nonreducible 5′ end extended construct could be overcome by incorporation of the disulfide linker. The passenger strand extended constructs without backbone strand (SS-siRNA/3′ov, SS-siRNA/5′ov) even outperformed their nonreducible equivalents.

The silencing for the outstanding structures had reached a level that made it hard to draw conclusions on the effect of the bioreducible attachment of the siRNA or the larger stepwise-extended structures. Therefore, the best performing constructs were further compared by determining their EC_{50} values (**Supplementary Figures S4** and **S5**). The difference between the structures remained nonsignificant with the following exceptions. The EC_{50} value of SS-1bb1si/3′ov (19.9 nM) was approximately twofold higher than the EC_{50} value of the remaining structures containing the 79-nucleotide backbone strand. In case of the step-by-step extended siRNA, Ext IV (181 nucleotides, EC_{50} of 4.4 nM) performed significantly better than Ext II (99 nucleotides, EC_{50} of 11.7 nM) for which luciferase knockdown was already saturated at 0.2 µM siRNA. None of the structures led to a significant decrease in metabolic activity as determined at a siRNA concentration of 0.2 µM with MTT(3-(4,5-dimethylthiazol-2-yl)-2,5-diphenyltetrazolium bromide) assay (**Supplementary Figure S6**). No significant luciferase knockdown was observed when the eGFP-siRNA was replaced with a control siRNA for the bioreducible constructs (**Supplementary Figure S7**). Hence, the reduced luciferase expression can be attributed to RNAi-mediated knockdown.

Polyplex stability analysis by agarose gel retardation assay revealed no major differences between the larger structures (**Supplementary Figure S8**). Dynamic light scattering measurements revealed that polyplexes of polymer 689 and the siRNA constructs present heterogeneous populations of nanoparticles with sizes in the submicrometer range and high polydispersity indices (**Supplementary Table S2**). Like for many related cationic carriers, probably multiple thousands

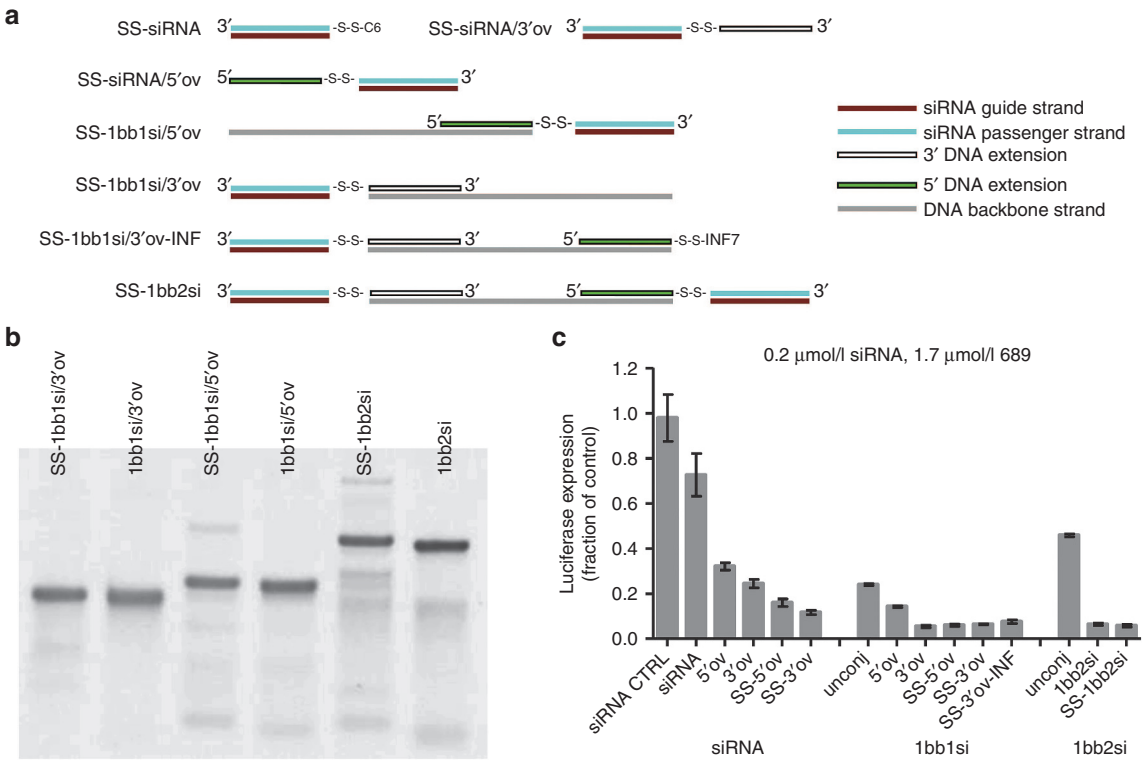

Figure 6. Bioreducible conjugation of the siRNA to the DNA backbone using disulfide chemistry. (**a**) Schematic representation of the structures from previous experiments with a disulfide linker introduced between the 5′ passenger strand and the DNA extension. For SS-1bb1si/3′ov-INF, influenza peptide 7 is conjugated to the 5′ DNA extension via its cysteine. (**b**) Verification of correct assembly by native polyacrylamide gel electrophoresis (gel cropped). (**c**) Transfection efficiency of the disulfide containing constructs.

of siRNAs are aggregated into the several hundred nanometer polyplexes. Thus the lack of significant size differences between the different siRNA constructs is not surprising.

Different polycations for siRNA transfection

So far, polymer 689 was used to test the effect of DNA extension of siRNA on transfection efficiency. It is also of interest if these findings hold true for more commonly used transfection agents like polyethyleneimine (PEI), or for lipid-containing formulations such as lipopolymer 454. The latter contains six tyrosines and two oleic acid units, which provide excellent stabilization through hydrophobic interactions and endosomal lysis through membrane destabilization. The fatty acid unit is connected to two identical arms consisting of two Stp units, three tyrosines for stabilization, and a terminal cysteine (**Supplementary Figure S9**).[39]

Hence, siRNA, 1bb2si, and 1bb2si-unconj were complexed with linear PEI and lipopolymer 454 at two different polymer concentrations (corresponding to N/P ratio of 6 for siRNA and 1bb2si, respectively) and tested for gene silencing efficiency (**Supplementary Figure S10**) and metabolic activity (**Supplementary Figure S11**) in N2A/eGFPLuc cells. Polyplexes formed with linear PEI and canonical siRNA worked at neither concentration, while polyplexes formed with linear PEI and 1bb2si mediated gene silencing (**Supplementary Figure S10** left) to some extent. In contrast, if the well-stabilizing lipopolymer 454 was used for complexation, canonical siRNA already exhibited an efficient knockdown (82%), which could not be achieved by 1bb2si (60%). Both constructs were compared at their optimum polymer concentration (3.9 µM for siRNA, 9.2 µM for 1bb2si) (**Supplementary Figure S10** right).

Consequently one can assume that the findings for polymer 689 can be translated to other polycationic transfection agents such as PEI lacking lipidic moieties. For lipid-containing delivery agents, the additional stabilizing effect of the DNA extensions appears not to be necessary or even counterproductive.

Attachment of functional domains to siRNA

Stabilization of siRNA polyplexes is only one requirement for successful nucleic acid delivery. Receptor targeting for improved and specific intracellular uptake[8,40] and transport across the endolysosomal barrier[41,42] are additional steps where functionalization can be beneficial. Disulfide chemistry provides the option to attach other functional units through the DNA backbone strand to the siRNA. INF-7 is a lytic peptide known to promote endosomal escape.[37] It was coupled to the 3′ thiol–modified DNA extension sequence by the peptide's N-terminal cysteine. A construct containing one 5′ passenger strand extended siRNA connected via the DNA backbone to INF-7 was assembled as previously described (SS-1bb1si/3′ov-INF) (**Figure 7a**). As expected, after complexation with polymer 689, the inclusion of INF-7 had no advantage over the respective construct without INF-7 (SS-1si1bb/3′ov) (**Figure 6c**). The histidines of polymer 689 already promote sufficient endosomal escape. Hence,

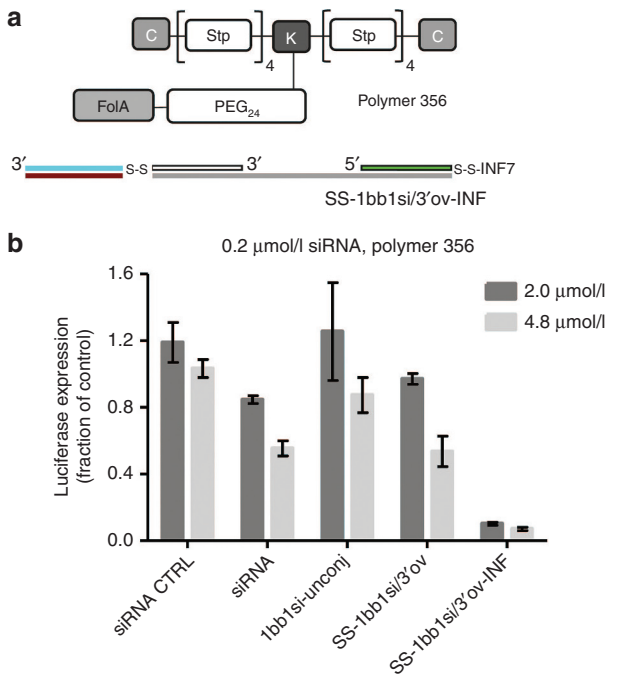

Figure 7. Conjugation of INF-7 to siRNA via a DNA backbone strand. (**a**) Polymer 356 for complexation of SS-1bb1si/3′ov-INF (C: cysteine; Stp: succinoyl tetraethylene pentamine; K: lysine; PEG_{24}: polyethylene glycol consisting of 24 ethylene glycol units; FolA: folic acid) and schematic representation of SS-1bb1si/3′ov-INF. (**b**) Transfection efficiency of siRNA hybridized to the DNA backbone strand with (SS-1bb1si/3′ov-INF) and without INF-7 (SS-1bb1si/3′ov).

polymer 356, lacking histidines, was used to verify a positive effect of INF-7 as part of the nanostructure (**Figure 7a**).

Polymer 356 is a three-armed polymer of which two arms contain positively charged Stp units and terminal cysteines for polyplex stabilization. The third arm contains 24 ethylene glycol units (PEG_{24}) for shielding and enhanced solubility and, in addition, folic acid to promote specific cellular uptake in folate receptor–expressing cells.[43]

The polyplexes were incubated on folate receptor–positive KB/eGFPLuc cells with an incubation time of 1 hour and a siRNA concentration of 0.2 µM. Indeed, SS-1bb1si/3′ov-INF showed a great increase in silencing over SS-1bb1si/3′ov and canonical siRNA without reduction in metabolic activity as part of a highly functional folate-targeted and PEG-shielded polyplex (**Figure 7b** and **Supplementary Figure S12**). Folate receptor targeting was verified by testing the formulation in a ligand competition assay using folate-containing medium (**Supplementary Figure S13**). In addition, lack of gene silencing by using ligand-free polymer 188 was demonstrated (**Supplementary Figure S13**). This proves that functional units can be attached to siRNA in a very simple way via a tunable DNA adaptor that improves polyplex stability itself (**Supplementary Figure S14**).

Discussion

This study demonstrates how siRNA can be extended by DNA adaptors to improve complex formation with sequence-defined cationic polymers, resulting in improved gene silencing efficiency. We tested several DNA/siRNA nanostructures ranging from DNA extension of one siRNA up to structures where two to ten siRNA units are merged into one construct. Delivery could be improved remarkably after complexation with a three-armed cationic polymer. Interestingly, the larger structures containing multiple siRNAs were less potent than the simple ones with one or two siRNA units. The observed key criterion for efficacy was the simple extension of siRNA with DNA to provide a sufficient number of negative charges.

We could figure out in a step-by-step extension of a single siRNA that a prolongation of up to 181 DNA nucleotides results in a significant improvement of transfection efficiency.

An additional finding was that a 3′ DNA extended siRNA passenger strand is advantageous over a 5′ extended one. We speculate that 5′ DNA extensions disturb RISC loading or passenger strand removal. We can exclude differences in secondary structure of the DNA extension being responsible for this effect as this observation is also present when the extension is hybridized to a DNA backbone strand. So when conjugating siRNA to DNA, the 3′ end of the passenger strand should be chosen as attachment site.

This fact indicates that steric hindrance is an issue to consider. To overcome this limitation, we introduced a reducible disulfide linker between the 5′ siRNA passenger strand and the DNA extension, which should liberate the siRNA from the DNA adaptor in the cytosol. With this strategy, it was possible to enhance the performance of the 5′ extension constructs to the level of their 3′ counterparts. Hence if siRNA should be modified on both ends of the passenger strand, a reducible conjugation should be considered for the 5′ terminus.

Eventually, we could lift these findings to a more general level as DNA extension of siRNA is also beneficial when using linear PEI as transfection agent. This is well in agreement with the previous finding showing enhanced activity of linear PEI when using sticky siRNA.[15] In contrast, when lipopolymer 454 was used containing both fatty acids and tyrosines for polyplex stabilization,[39] transfection efficiency could not be further improved by siRNA extensions. The already known high siRNA polyplex stability apparently makes an additional stabilizing effect by DNA extended siRNAs dispensable.

Importantly, we also showed that a DNA backbone strand cannot only be used for extension or connection of multiple siRNAs but also to include other functional domains in a very simple way. Thiolated DNA extensions can be conjugated to any thiol-containing functional molecule. Through hybridization with the DNA backbone strand, the functional unit can be linked to siRNA. As a proof of concept, we conjugated the endosomolytic peptide INF-7 via a 79-nucleotide DNA backbone strand to siRNA. The INF-7–modified DNA backbone strand, which can be further optimized in terms of length and structure for each application, improved transfection efficiency and polyplex stability with the multifunctional polymer 356.

This strategy resulted in a straightforward construction of defined folate receptor–targeted siRNA polyplexes, containing all key elements for functional delivery, including particle surface shielding by PEG, bioreversible stabilization by disulfide bonding, folate as receptor-targeting ligand, and INF-7 for endosomal escape.

Materials and methods

Assembly of the constructs. All DNA sequences used in this work were designed with NUPACK.[44] The constructs were assembled in assembly buffer (10 mM Tris-Cl; 5 mM $MgCl_2$; pH 7.5) to yield a concentration of 1–6 µM. The components were mixed in their respective molar amount, incubated at 95 °C for 5 minutes, and cooled to RT at a rate of ca. 2 °C/minute. We used eGFP-siRNA with a chemically modified guide strand (g: UGCUUGUCGGCcAUGAuAUdTsdT, Axolabs, Kulmbach, Germany) and dependent on the experiment one of the following passenger strands: p5′: dGdCdCdGdGdAdTdCdGd CdCdAdCdAdTdAdAdCAuAucAuGGccGAcAAGcA-dTsdT; p3′: AuAucAuGGccGAcAAGcAdTsdTdCdGdAdCdGdGdAd TdAdTdAdCdAdTdG-dAdCdG; pSS: C6SSC6-AuAucAuGG ccGAcAAGcAdTsdT; and a siCTRL control sequence (g: CuAAuAcAGGCcAAuAcAUdTsdT; p: C6SSC6-AuGuAuuGG ccuGuAuuAGdTsdT; Axolabs). Upper case letters A, C, G, and U represent RNA nucleotides, lower case letters a, c, g, and u are 2'-O-methyl-nucleotides, dA, dC, dG, and dT code for DNA nucleotides, and s represents a phosphorothioate linkage. C6SSC6 is a symmetrical hexyl-disulfide linker. The DNA backbone strands were purchased from Sigma Aldrich (Hamburg, Germany).

Purification with high pressure liquid chromatography. Purification of the DNA extensions coupled via a disulfide bond to the siRNA passenger strand or INF-7 was performed with high pressure liquid chromatography (VWR Hitachi Chromaster consisting of 5430 Diode array detector and 5160 gradient pump, Darmstadt, Deutschland). The products were separated with a waters XTerra C8 column (5 µm, 4.6×150 mm, Waters, Eschborn, Germany) and eluted with an acetonitrile /0.1 M triethylammonium acetate gradient (95:5 to 35:65 in 30 minutes). The collected fractions were lyophilized and stored at –20 °C.

Coupling of DNA extensions to siRNA passenger strands via a disulfide bond. Disulfide-modified siRNA was reduced with buffered tris(2-carboxyethyl)phosphine (700 times molar excess, Sigma Aldrich) for 2.5 hours at RT. Tris(2-carboxyethyl)phosphine was removed by EtOH precipitation. The remaining pellet was activated with 2.5 mM 5,5′-dithiobis-(2-nitrobenzoic acid) (DTNB, 17 times molar excess, Sigma Aldrich) for 1 hour at RT. The activated siRNA was purified by EtOH precipitation and dissolved in 20 mM 4-(2-hydroxyethyl)-1-piperazineethanesulfonic acid, pH 8.4. The absence of dimers was verified with native PAGE. Disulfide-modified DNA extensions were reduced with buffered tris(2-carboxyethyl)phosphine (700 times excess), purified by EtOH precipitation, and dissolved in 4-(2-hydroxyethyl)-1-piperazineethanesulfonic acid buffer. The activated siRNA and the reduced DNA extensions were combined at a concentration of 50 µM and incubated at RT for 1 hour. Reaction was completed upon standard freezing to –20 °C, presumably facilitated by the temporarily high concentrations in the mother liquor. The products were purified by EtOH precipitation and high pressure liquid chromatography. Their correct size and purity were verified by native PAGE.

Coupling of DNA extension strands to INF-7. The cysteine of the INF-7 peptide (GLFE AIEG FIEN GWEG MIDG WYGC)[37] was activated with DTNB (17 times molar excess) and purified by high pressure liquid chromatography. The product was incubated with thiolated DNA extension in 20 mM 4-(2-hydroxyethyl)-1-piperazineethanesulfonic acid pH 8.4 for 1 hour at RT and frozen to –20 °C. The product was again purified by high pressure liquid chromatography and verified by agarose gel electrophoresis.

Polyplex formation. Sequence-defined polymers 689, 356 and lipopolymer 454 were synthesized by solid phase–assisted synthesis as described in our previous publications.[33,39,43] The siRNA and the required amount of polymer were separately diluted in 20 mM 4-(2-hydroxyethyl)-1-piperazineethanesulfonic acid-buffered 5% glucose pH 7.4 in a final volume of 10 µl. Both solutions were pooled and incubated for 45 minutes at RT.

Cell culture. Murine neuroblastoma (N2A/eGFPLuc) or human cervix carcinoma (KB/eGFPLuc) cells, each stably transfected with an enhanced green fluorescent protein GL3 firefly luciferase fusion protein,[40,43,45] were cultured at 37 °C in Dulbecco's modified Eagle's Medium with 1 g/l glucose (for N2A), or folate-free Roswell Park Memorial Institute 1640 medium (for KB), respectively, in both cases supplemented with 10% FBS, 4 mM glutamine, 100 U/ml penicillin, and 100 µg/ml streptomycin (Life Technologies, Darmstadt, Germany). For maintenance, the cells were detached with a trypsin-ethylenediaminetetraacetic acid solution (0.25%) and seeded at the desired concentration.

Transfection. N2A/eGFPLuc or KB/eGFPLuc cells were seeded in 96-well plates in 100 µl medium (N2A/eGFPLuc: 5,000 cells per well in Dulbecco's modified Eagle's Medium, 1g/l glucose, 10% FBS, KB/eGFPluc: 4,000 cells per well in folate-free Roswell Park Memorial Institute 1640 medium, 10% FBS). After 24 hours, the medium was exchanged with 80 µl of fresh medium. The formed polyplexes containing the eGFP-siRNA for downregulation of the eGFP–luciferase fusion protein were added in a volume of 20 µl to each well. After the desired incubation time, the medium was exchanged with 100 µl fresh medium. Forty-eight hours after the transfection, the cells were incubated with 100 µl of lysis buffer (25 mM Tris, pH 7.8, 2 mM ethylenediaminetetraacetic acid, 2 mM 1,4-dithiothreitol, 10% glycerol, 1% Triton X-100). Thirty-five microliters of the lysate was used for luciferase activity determination with a luciferase assay kit (100 ml of Luciferase Assay Buffer, Promega, Mannheim, Germany) in a luminometer (Centro LB 960 plate reader luminometer, Berthold Technologies, Bad Wildbad, Germany).

siRNA binding assay. siRNA (500 ng) or siRNA/DNA conjugate and the amount of polymer corresponding to the required N/P ratio were diluted separately in 20 mM HEPES-buffered 5% glucose, pH 7.4 in a volume of 10 µl. The solutions were pooled and incubated at RT for 45 minutes. After addition of 4 µl of loading buffer (prepared from 6 ml of glycerine, 1.2 ml of 0.5 M ethylenediaminetetraacetic acid, 2.8 ml of H_2O, 0.02 g of bromophenol blue), the polyplexes were run on a 1.5% agarose gel at 90 V for 45 minutes.

MTT assay. Cells were transfected in 96-well plates as described earlier. Forty-eight hours after transfection, 10 µl

of MTT solution (3-(4,5-dimethylthiazol-2-yl)-2,5-diphenyltetrazolium bromide) were added to a final concentration of 0.5 mg/ml. The plate was incubated at 37 °C for 2 hours for formation of the insoluble purple formazan. The medium was removed, and the plate was stored at –80 °C for at least 1 hour. Hundred microliters of dimethyl sulfoxide was added to each well which dissolved the formazan and was quantified through its absorbance at 530 nm using a microplate reader (Tecan Spectrafluor Plus, Tecan, Männedorf, Switzerland). Results are presented relative to buffer treated control cells.

Acknowledgments This work was supported by the DFG Collaborative Research Centre 1032 project B4 and the Excellence Cluster "Nanosystems Initiative Munich". The authors declared no conflict of interest.

Supplementary material

Table S1. Sequences.
Table S2. Particle sizes measured by dynamic light scattering.
Figure S1. Assembly of star-shaped multi-siRNA.
Figure S2. Gene silencing of the star-shaped multi-siRNAs.
Figure S3. Influence of single-stranded (ss) and double-stranded (ds) domains on transfection efficiency.
Figure S4. Dose–response curves for EC_{50} value determination.
Figure S5. EC_{50} values for best performing constructs with polymer 689.
Figure S6. Metabolic activity assay with polymer 689.
Figure S7. Specificity of eGFP–luciferase knockdown demonstrated by nanostructures containing a control siRNA instead of eGFP-siRNA.
Figure S8. Polyplex stability for all constructs as determined by a nucleic acid gel retardation assay.
Figure S9. Schematic representation of lipopolymer 454.
Figure S10. Transfection efficiency after complexation with linear PEI and lipopolymer 454.
Figure S11. Metabolic activity assays with linear PEI and lipopolymer 454.
Figure S12. Metabolic activity assay of the INF-7 conjugate.
Figure S13. Folate targeting of SS-1bb1si/3′ov-INF with polymer 356.
Figure S14. Binding assay for canonical siRNA and 1bb2si with polymer 356.

References

1. Fire, A, Xu, S, Montgomery, MK, Kostas, SA, Driver, SE and Mello, CC (1998). Potent and specific genetic interference by double-stranded RNA in Caenorhabditis elegans. *Nature* **391**: 806–811.
2. Bartel, DP (2004). MicroRNAs: genomics, biogenesis, mechanism, and function. *Cell* **116**: 281–297.
3. Elbashir, SM, Harborth, J, Lendeckel, W, Yalcin, A, Weber, K and Tuschl, T (2001). Duplexes of 21-nucleotide RNAs mediate RNA interference in cultured mammalian cells. *Nature* **411**: 494–498.
4. Lee, RC, Feinbaum, RL and Ambros, V (1993). The *C. elegans* heterochronic gene lin-4 encodes small RNAs with antisense complementarity to lin-14. *Cell* **75**: 843–854.
5. Whitehead, KA, Langer, R and Anderson, DG (2009). Knocking down barriers: advances in siRNA delivery. *Nat Rev Drug Discov* **8**: 129–138.
6. Aigner, A (2011). MicroRNAs (miRNAs) in cancer invasion and metastasis: therapeutic approaches based on metastasis-related miRNAs. *J Mol Med (Berl)* **89**: 445–457.
7. Kota, J, Chivukula, RR, O'Donnell, KA, Wentzel, EA, Montgomery, CL, Hwang, HW *et al.* (2009). Therapeutic microRNA delivery suppresses tumorigenesis in a murine liver cancer model. *Cell* **137**: 1005–1017.
8. Lächelt, U and Wagner, E (2015). Nucleic acid therapeutics using polyplexes: a journey of 50 years (and beyond). *Chem Rev* **115**: 11043–11078.
9. Sakurai, Y, Hatakeyama, H, Sato, Y, Hyodo, M, Akita, H and Harashima, H (2013). Gene silencing via RNAi and siRNA quantification in tumor tissue using MEND, a liposomal siRNA delivery system. *Mol Ther* **21**: 1195–1203.
10. Wagner, E (2012). Polymers for siRNA delivery: inspired by viruses to be targeted, dynamic, and precise. *Acc Chem Res* **45**: 1005–1013.
11. Boussif, O, Lezoualc'h, F, Zanta, MA, Mergny, MD, Scherman, D, Demeneix, B *et al.* (1995). A versatile vector for gene and oligonucleotide transfer into cells in culture and in vivo: polyethylenimine. *Proc Natl Acad Sci U S A* **92**: 7297–7301.
12. Pinel, S, Aman, E, Erblang, F, Dietrich, J, Frisch, B, Sirman, J *et al.* (2014). Quantitative measurement of delivery and gene silencing activities of siRNA polyplexes containing pyridylthiourea-grafted polyethylenimines. *J Control Release* **182**: 1–12.
13. Scholz, C and Wagner, E (2012). Therapeutic plasmid DNA versus siRNA delivery: common and different tasks for synthetic carriers. *J Control Release* **161**: 554–565.
14. Allison, SJ and Milner, J (2014). RNA interference by single- and double-stranded siRNA with a DNA extension containing a 3' nuclease-resistant mini-hairpin structure. *Mol Ther Nucleic Acids* **2**: e141.
15. Bolcato-Bellemin, AL, Bonnet, ME, Creusat, G, Erbacher, P and Behr, JP (2007). Sticky overhangs enhance siRNA-mediated gene silencing. *Proc Natl Acad Sci U S A* **104**: 16050–16055.
16. Lee, SH, Mok, H, Jo, S, Hong, CA and Park, TG (2011). Dual gene targeted multimeric siRNA for combinatorial gene silencing. *Biomaterials* **32**: 2359–2368.
17. Mok, H, Lee, SH, Park, JW and Park, TG (2010). Multimeric small interfering ribonucleic acid for highly efficient sequence-specific gene silencing. *Nat Mater* **9**: 272–278.
18. Brunner, K, Harder, J, Halbach, T, Willibald, J, Spada, F, Gnerlich, F *et al.* (2015). Cell-penetrating and neurotargeting dendritic siRNA nanostructures. *Angew Chem Int Ed Engl* **54**: 1946–1949.
19. Chang, CI, Lee, TY, Kim, S, Sun, X, Hong, SW, Yoo, JW *et al.* (2012). Enhanced intracellular delivery and multi-target gene silencing triggered by tripodal RNA structures. *J Gene Med* **14**: 138–146.
20. Nakashima, Y, Abe, H, Abe, N, Aikawa, K and Ito, Y (2011). Branched RNA nanostructures for RNA interference. *Chem Commun (Camb)* **47**: 8367–8369.
21. Hong, CA, Jang, B, Jeong, EH, Jeong, H and Lee, H (2014). Self-assembled DNA nanostructures prepared by rolling circle amplification for the delivery of siRNA conjugates. *Chem Commun (Camb)* **50**: 13049–13051.
22. Hong, CA, Eltoukhy, AA, Lee, H, Langer, R, Anderson, DG and Nam, YS (2015). Dendrimeric siRNA for efficient gene silencing. *Angew Chem Int Ed Engl* **54**: 6740–6744.
23. Tam, DY and Lo, PK (2015). Multifunctional DNA nanomaterials for biomedical applications. *J Nanomaterials* **2015**: 765492.
24. de Vries, JW, Zhang, F and Herrmann, A (2013). Drug delivery systems based on nucleic acid nanostructures. *J Control Release* **172**: 467–483.
25. Chang, M, Yang, CS and Huang, DM (2011). Aptamer-conjugated DNA icosahedral nanoparticles as a carrier of doxorubicin for cancer therapy. *ACS Nano* **5**: 6156–6163.
26. He, Y, Ye, T, Su, M, Zhang, C, Ribbe, AE, Jiang, W *et al.* (2008). Hierarchical self-assembly of DNA into symmetric supramolecular polyhedra. *Nature* **452**: 198–201.
27. Goodman, RP, Berry, RM and Turberfield, AJ (2004). The single-step synthesis of a DNA tetrahedron. *Chem Commun* **12**: 1372–1373.
28. Andersen, ES, Dong, M, Nielsen, MM, Jahn, K, Subramani, R, Mamdouh, W *et al.* (2009). Self-assembly of a nanoscale DNA box with a controllable lid. *Nature* **459**: 73–76.
29. Rothemund, PWK (2006). Folding DNA to create nanoscale shapes and patterns. *Nature* **440**: 297–302.
30. Saccà, B and Niemeyer, CM (2012). DNA origami: the art of folding DNA. *Angew Chem Int Ed Engl* **51**: 58–66.
31. Kocabey, S, Meinl, H, MacPherson, IS, Cassinelli, V, Manetto, A, Rothenfusser, S *et al.* (2014). Cellular uptake of tile-assembled DNA nanotubes. *Nanomaterials* **5**: 47–60.
32. Lee, H, Lytton-Jean, AK, Chen, Y, Love, KT, Park, AI, Karagiannis, ED *et al.* (2012). Molecularly self-assembled nucleic acid nanoparticles for targeted *in vivo* siRNA delivery. *Nat Nanotechnol* **7**: 389–393.
33. Schaffert, D, Troiber, C, Salcher, EE, Fröhlich, T, Martin, I, Badgujar, N *et al.* (2011). Solid-phase synthesis of sequence-defined T-, i-, and U-shape polymers for pDNA and siRNA delivery. *Angew Chem Int Ed Engl* **50**: 8986–8989.
34. Lächelt, U, Wittmann, V, Müller, K, Edinger, D, Kos, P, Höhn, M *et al.* (2014). Synthetic polyglutamylation of dual-functional MTX ligands for enhanced combined cytotoxicity of poly(I:C) nanoplexes. *Mol Pharm* **11**: 2631–2639.
35. Nie, Y, Günther, M, Gu, Z and Wagner, E (2011). Pyridylhydrazone-based PEGylation for pH-reversible lipopolyplex shielding. *Biomaterials* **32**: 858–869.
36. Kos, P, Lächelt, U, Herrmann, A, Mickler, FM, Döblinger, M, He, D *et al.* (2015). Histidine-rich stabilized polyplexes for cMet-directed tumor-targeted gene transfer. *Nanoscale* **7**: 5350–5362.
37. Plank, C, Oberhauser, B, Mechtler, K, Koch, C and Wagner, E (1994). The influence of endosome-disruptive peptides on gene transfer using synthetic virus-like gene transfer systems. *J Biol Chem* **269**: 12918–12924.
38. Lächelt, U, Kos, P, Mickler, FM, Herrmann, A, Salcher, EE, Rödl, W *et al.* (2014). Fine-tuning of proton sponges by precise diaminoethanes and histidines in pDNA polyplexes. *Nanomedicine* **10**: 35–44.

39. Troiber, C, Edinger, D, Kos, P, Schreiner, L, Kläger, R, Herrmann, A *et al.* (2013). Stabilizing effect of tyrosine trimers on pDNA and siRNA polyplexes. *Biomaterials* **34**: 1624–1633.
40. Dohmen, C, Fröhlich, T, Lächelt, U, Röhl, I, Vornlocher, HP, Hadwiger, P *et al.* (2012). Defined folate-PEG-siRNA conjugates for receptor-specific gene silencing. *Mol Ther Nucleic Acids* **1**: e7.
41. Wagner, E (1998). Effects of membrane-active agents in gene delivery. *J Control Release* **53**: 155–158.
42. Boeckle, S, Fahrmeir, J, Roedl, W, Ogris, M and Wagner, E (2006). Melittin analogs with high lytic activity at endosomal pH enhance transfection with purified targeted PEI polyplexes. *J Control Release* **112**: 240–248.
43. Dohmen, C, Edinger, D, Fröhlich, T, Schreiner, L, Lächelt, U, Troiber, C *et al.* (2012). Nanosized multifunctional polyplexes for receptor-mediated siRNA delivery. *ACS Nano* **6**: 5198–5208.
44. Zadeh, JN, Steenberg, CD, Bois, JS, Wolfe, BR, Pierce, MB, Khan, AR *et al.* (2011). NUPACK: analysis and design of nucleic acid systems. *J Comput Chem* **32**: 170–173.
45. Fröhlich, T, Edinger, D, Kläger, R, Troiber, C, Salcher, E, Badgujar, N *et al.* (2012). Structure-activity relationships of siRNA carriers based on sequence-defined oligo (ethane amino) amides. *J Control Release* **160**: 532–541.

Supplementary Information accompanies this paper on the Molecular Therapy–Nucleic Acids website (http://www.nature.com/mtna)